Earth Surf. Dynam. Discuss., https://doi.org/10.5194/esurf-2018-15
Manuscript under review for journal Earth Surf. Dynam.
Discussion started: 28 February 2018

Mechanical State of Gravel Soil in Mobilization of Rainfall-Induced Landslide in Wenchuan seismic area, Sichuan province, China

Liping Liao[1, 2, 3], Yunchuan Yang[1, 2, 3], Zhiquan Yang[4], Yingyan Zhu[5*], Jin Hu[5], D.H.Steve Zou[6]

[1]College of Civil Engineering and Architecture, Guangxi University, Nanning 530004, China
[2]Key Laboratory of Disaster Prevention and Structural Safety of Ministry of Education, Guangxi University, Nanning 530004, China
[3]Guangxi Key Laboratory of Disaster Prevention and Engineering Safety, Guangxi University, Nanning 530004, China
[4]Faculty of Land Resource Engineering, Kunming University of Science and Technology, Kunming 650500, China
[5]Institute of Mountain Hazards and Environment, Chinese Academy of Sciences and Ministry of Water Conservancy, Chengdu 610041, China
[6]Department of Civil and Resource Engineering, Dalhousie University, Halifax, NS, Canada B3H4K5
Correspondence to: Y. Y. Zhu (zh_y_y_imde@163.com)

Abstract Although gravel soils generated by seismic shaking in Wenchuan earthquake area have subjected to natural consolidation process for nearly ten years, geological hazards, such as slope failures with ensuing landslides, frequently are haunting the area. In this paper, artificial flume model tests and triaxial tests were used to make close observation on the mechanical state of gravel soil in Wenchuan seismic area. The results showed that: (1) The timing and patterns of landslide initiations were closely related to their initial dry densities, and the initiation processes were accompanied with a variation of dry density and void ratio; (2) Fine particle migration in soil and coarse-fine particle content rearrangement contributed to the internal micro structure reorganization, which was supposed to be the main reason for variation of dry density and void ratio; (3) Gravel soils with unchanged grain compositions, if under the same hydrostatic compression, they approached to an identical critical void ratio to fail; (4) The mechanical state of certain sort of gravel soil can be identified by its relative position between state parameter (e, p') and e_c-p' planar critical state line; (5) Gravel soil slope failed and then evolved into landslide under lasting rainfall leaching, while in gravel slope there co-existed soil dilatation and contraction, but the dilatation was dominant. Above research findings not only could be used to interpret landslide initiation but also would provide an insight for landslide warning forecast of gravel slope in seismic area.

Keywords Mechanical state • gravel soil• landslide• critical state• Wenchuan seismic area

1 Introduction

In 2008, gravel soils generated by seismic shaking in Wenchuan earthquake area contributed to the large number of loose deposits (Tang and Liang 2008; Xie et al., 2009). These deposits characterized by wide grading, under-consolidation and low density, were locating at the both sides of highway and gully, and resulted in the formation of soil slopes (Cui et al., 2010; Qu et al., 2012; Zhu et al., 2011). Although gravel soils have subjected to natural consolidation process for nearly ten years, geological hazards, such as slope failures with ensuing landslides, are readily to motivate when it suffers heavy rainfall and frequently are haunting the local region which caused intense gully erosion, severe damages of the Duwen highway, and huge losses of life and property (Chen et al., 2012a; Chen et al., 2017; Cui et al., 2013; Hu et al., 2016; Hu et al., 2014; Huang et al., 2012; Huang and Tang 2014; Li et al., 2010; Liu et al., 2016; Ma et al., 2013; Ni et al., 2014; Sun et al., 2011; Tang et al., 2012; Tang et al., 2011b; Tang et al., 2009; Wang et al., 2015; Xu et al., 2012; Yin et al., 2016; You et al., 2012; Zhang and Zhang 2017; Zhang et al., 2013; Zhang et al., 2014; Zhou et al., 2015; Zhou and Tang 2013; Zhou et al., 2014; Zhuang et al., 2012).

Fully understanding the mechanical state of gravel soil is an engineering and scientific basis for disaster prevention and mitigation in a seismic area (Chen et al., 2010). Generally, the void ratio of soil is an important parameter in describing the mechanical state quantitatively (Been and Jefferies 1985), which has already involved the deterministic analysis of the critical state of soil, and belongs to an important branch of soil mechanics - the critical state soil mechanics (Schofield and Wroth 1968).

The critical state soil mechanics indicated that soil must experience the transformation process of a relatively steady condition into the critical state (Schofield and Wroth 1968). In 1936, Casagrande (1936) pointed out that the critical state was that loose soil contracted, and dense soil dilated to the same critical void ratio in the drained shearing test. Some of the observed phenomena of landslides might be approximately explained by the critical state soil mechanics (Fleming et al., 1989; Sassa 1984; Wang and Sassa 2003), thus since the 1980s, the critical state of soil had been introduced into the initiation mechanism of the landslide and debris flow, which had received extensive attentions (Fleming et al., 1989; Sassa 1984; Verdugo and Ishihara 1996; Wang and Sassa 2003; Gabet and Mudd 2006; Iverson et al., 2010; Iverson 2000; Iverson 2005; Iverson et al., 2000; Iverson et al., 1997; Schulz et al., 2009). Wherein, in 1984, Sassa (1984) concluded that the liquefaction of loose sand was attributed to the critical state; in addition, due to the incompressibility of water, the dilation and contraction behavior of the soil resulted in the fluctuation of pore pressure in the undrained conditions. Based on the F line drawn by Casagrande(1936), in 1989, Fleming (1989) found that the increase of pore water pressure corresponded to the soil dilation and the intermittent debris flow; however, his research was in contrast to the theory proposed by Casagrande (1936) that "dilative soil was not easy to liquefy". In 1997, Iverson (1997) also found that the density of loose sand increased, and the density of dense sand decreased to the same critical density. His research can indirectly reflect the existence of the critical void ratio of soil. In 2000, Iverson et al (2000) demonstrated that in the shearing process of soil, the contractive behavior of the loose loamy sand prompted pore pressure to increase rapidly, which led to the immediate failure within the soil; in contrast, the dense loamy sand exhibited dilative behavior which resulted in the decrease of pore pressures. He also pointed out although it was not easy to observe the phenomenon that the landslide velocity depended on the void ratio, the void ratio played the important role in the formation of landslide. In his paper, the value of the critical void ratio was not mentioned. As the critical void ratio was a function of the mean effective stress (Verdugo and Ishihara 1996), based on the model of Iverson (2000) and critical sate soil mechanics (Schofield and Wroth 1968), the theoretical formula of the critical void ratio is deduced by Gabet and Mudd(2006). Besides, they pointed out the particle diameter of soils affected the rate at which the soil reaches a critical state; when the rainfall duration is sufficient for the dense soil to reach the critical void ratio, and to generate the excess pore pressure, the soil would dilate. This might be the reason for the

Earth Surf. Dynam. Discuss., https://doi.org/10.5194/esurf-2018-15
Manuscript under review for journal Earth Surf. Dynam.
Discussion started: 28 February 2018

paradoxical conclusion made by Fleming (1989). William (2009) found out the dilative strengthening might control the landslide velocity. In additon, other scholars also found that in the shearing process of soil, the critical state, the dilative and contractive behavior was exiting in residual soil, loess and coarse grained soil (Dai et al., 2000; Dai et al., 1999a; Dai et al., 1999b; Liu et al., 2012; Zhang et al., 2010; Zhu et al., 2005). Although the critical state soil mechanics had been applied to explain the mobilization of landslide theoretically since 1980s (Dai et al., 2000; Dai et al., 1999a; Dai et al., 1999b; Fleming et al., 1989; Gabet and Mudd 2006; Iverson et al., 2010; Iverson 2000; Iverson 2005; Iverson et al., 2000; Iverson et al., 1997; Liu et al., 2012; Sassa 1984; Schulz et al., 2009; Verdugo and Ishihara 1996; Wang and Sassa 2003; Zhang et al., 2010; Zhu et al., 2005), most precedent studies focus on the qualitative results and lack the field testing data. In addition, the critical state of gravel soil in a seismic area is not exactly identified in the field research. For example, is the mechanical state of gravel soil contraction or dilation? How to estimate the mechanical state of gravel soil when the landslide initiates?

Through artificial flume model tests and triaxial tests, this paper investigates the mechanical state of gravel soil in Niujuan valley, Yingxiu Town of Wenchuan County, Sichuan Province, China. More specially, first, the variation of soil moisture content and pore water pressure, and the macro-micro property was observed. Second, the mathematical expression of critical state of soil was proposed. Third, the mechanical state of gravel soil was discussed.

2 Field site and method

2.1 Field site

Niujuan Valley is locating in Yingxiu town of Wenchuan County, Sichuan Province, which is the epicenter of 12 May 2008 Wenchuan earthquake in China. The main valley of the basin has an area of 10.46km^2, and a length of 5.8km. The highest elevation is 2693m, and the largest relative elevation is 1833m. The range of the valley slope is 32.7%~52.5% (Tang and Liang 2008; Xie et al., 2009). Six small ditches are distributing in the basin. The valley is characterized by the abundant loose gravel soil, extremes of precipitous valley relief and the adequate rainfall, which contribute to the frequent landslides and debris flows with large scale. Hence, this valley is regarded as the most typical basin in the seismic area; and its excellent formative environment of landslide can provide the comprehensive reference model and the rich soil sample for the artificial flume model tests.

2.2 Soil tests and quantitative analysis

2.2.1 Artificial flume model test

Based on the field surveys along Duwen highway, Niujuan valley and the literature review (Chen et al., 2010; Fang et al., 2012; Tang et al., 2011a; YU et al., 2010), most of rainfall induced landslides is the shallow landslides, and the range of the slope gradient is 25°~40°; besides, the cumulative content of silt and clay (particle diameter < 0.075mm) is about 2%, which plays the important role in the mobilization of landslide and debris flow (Chen et al., 2010); the rainfall intensity triggering the landslides is 10mm/h~70mm/h. Considering the above basic data, the authors designed the artificial flume model, as shown in Fig. 1 (a). The length, width and height of the flume model are 300cm, 100cm and 100cm respectively.

The gravel soil samples are from Niujuan valley (Fig. 1 (b)). The specific gravity is 2.69. The minimum, the maximum dry density is 1.48g/cm^3 and 2.36g/cm^3; in addition, the minimum, the maximum void ratio is 0.14 and 0.82. The grading curve is shown in Fig. 1 (c). As shown in Fig. 1(c), the cumulative content of gravel (particle diameter < 2mm) is 30.74%, and the cumulative content of silt and clay (particle diameter < 0.075mm) is 2.78%. The model tests comprise of four initial dry densities: 1.54g/cm^3, 1.62g/cm^3, 1.72g/cm^3, 1.81g/cm^3 (Tab. 1), because the initial dry density influenced the formation of landslide (McKenna et al., 2011). In order to achieve a predetermined initial dry density, the soils of the models are divided into four layers and compacted. The thickness of each layer is 20cm, 15cm, 15cm and 10cm respectively (Fig. 1 (a)).

Artificial rainfall system, which was designed by the Institute of Soil and Water Conservation, CAS, comprises of two spray nozzles, a submersible pump, water box and a bracket. The range of nozzle sizes is 5~12mm, thus, the actual rainfall intensity in the field can be simulated. Three groups of sensors, including the micro-pore pressure sensors (model: TS-HM91, produced in England) and moisture sensors (model: SM300, produced in England), are placed between two layers of the soil to measure the volume water content and the pore water pressure (Fig. 1 (a)). DL2e device is applied to collect the data from the sensors, which can scan 30 channels within the same second, so that the time interval of data collection is set to one second.

2.2.2 Triaxial test

Triaxial tests were carried out on the dynamic triaxial apparatus in Institute of Mountain Hazards and Environment, CAS. The diameter and the height of sample were 15 cm and 30 cm (Fig. 2). The test is the saturated and consolidated drainage shear test at a shear rate of 0.8mm/minute, which comprise of two sets: the initial dry density of 1.94 and 2.00g/cm^3. The confining pressure is 50Kpa, 100Kpa and 150Kpa.

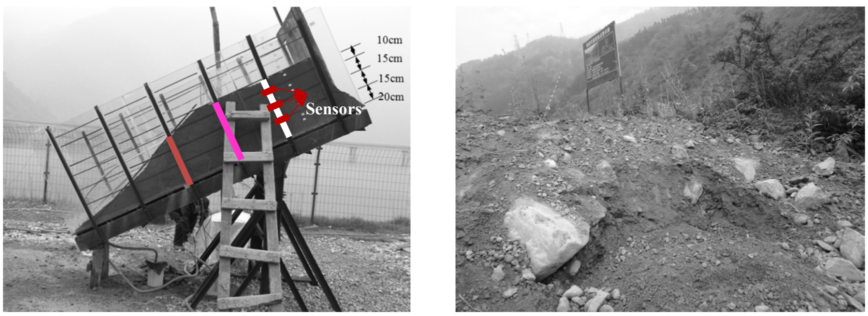

(a) Artificial flume model (the position of sampling: red line-1#, pink line-2#, white line-3#) (b) Gravel soil in Niujuan valley

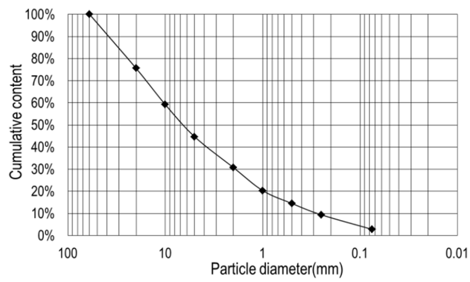

(c) Grain composition of gravel soil particle

Fig. 1 Test model and grain composition of gravel soil particle

Tab. 1 Sets of artificial flume soil model test

Factor / Number	Initial mass moisture content (%)	Gradient of slope (°)	Rainfall intensity (mm/h)	Initial dry density (g/cm^3)
1				1.54
2	6~8	27	47~50.2	1.62
3				1.72
4				1.81

Earth Surf. Dynam. Discuss., https://doi.org/10.5194/esurf-2018-15
Manuscript under review for journal Earth Surf. Dynam.
Discussion started: 28 February 2018

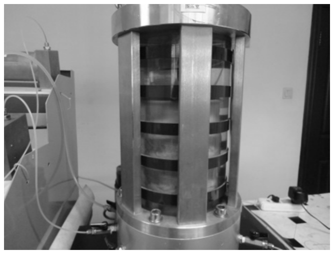

Fig. 2 Triaxial test equipment

2.2.3 Quantitative analysis method

Quantitative analysis is mainly based on artificial flume model test and triaxial test. Firstly, the state parameters of soil are expressed by the void ratio e and the mean effective stress p', which can be derived from the artificial flume model test. In artificial flume model test, at least three soil samples are collected by soil sampler in the same depth of the line 1#, 2# and 3#, and are used to calculate their natural density ρ, mass moisture content ω and dry density ρ_d. Later, void ratio can be calculated by the formula: $e=G_s/\rho_d-1$ (G_s is the specific gravity). The cumulative content of coarse P_5 (particle diameter > 5mm), gravel (particle diameter < 2mm) P_2, and silt and clay (particle diameter < 0.075mm) $P_{0.075}$ is obtained from the particle grading test. The mean effective stress p' is equal to one third of the sum of σ_x, σ_y and σ_z, wherein, the vertical stress σ_z is equal to γh, the horizontal stress σ_x and σ_y is equal to $K_a\gamma h$; h is the vertical distance between the some point inside the slope and the surface of the slope; β is the gradient of the slope; γ is the soil bulk density; K_a is the lateral pressure coefficient, which can be calculated by the formula (1) (Chen et al., 2012b); ϕ is the internal friction angle of soil. In this paper, β=27°, ϕ=33°.

$$K_a = \cos\beta \frac{\cos\beta - \sqrt{\cos^2\beta - \cos^2\phi}}{\cos\beta + \sqrt{\cos^2\beta - \cos^2\phi}} \quad (1)$$

Secondly, the critical state line (CSL, e_c-lnp') is derived from the saturated and consolidated drainage shear test. Finally, based on the critical state soil mechanics, according to the relative position of the state parameter (e, p') at the CSL, the mechanical state of the soil can be estimated. When the soil state (e, p') is located at the upper right of the CSL, the soil is contracted. When the soil state (e, p') is located at the lower left of the CSL, the soil is dilated (Casagrande A 1936; Schofield and Wroth 1968).

3 Results

3.1 Soil moisture content and pore water pressure

As shown in Fig.3~Fig.6, the variation of the volume moisture content of soil depth of 10~25cm exhibits the similar tendency, which includes the constant state since the beginning of rainfall, the rapid increase when the rainfall seeping into soil, and the steady growth trend at the end. However, throughout the rainfall, the volume moisture content of soil depth of 40cm exhibits a slow-growth trend or remains the stable. For example, when the dry density is 1.54g/cm^3, at the beginning of rainfall, the volume moisture contents of three depths all remain the same. When the rainfall duration is about 500s, the volume moisture content of soil depth of 10cm begins to increase fast, while the volume moisture content of soil depth of 25cm~40cm still remains unchanged. When the rainfall duration is about 1200s, as the rainfall penetrates into the internal soil, the volume moisture content of soil depth of 25cm begins to increase suddenly, while the volume moisture content of soil depth of 10cm maintains a slow changing trend. Besides, the variation of pore water pressure shows the similar trend which is characterized by a sharp increase at first, then decreases rapidly and the continuous dynamic fluctuation. The pore water pressure of soil depth of 10~25cm is mostly positive, while when the initial dry density is 1.81g/cm^3, the pore water pressure of soil depth of 40cm changes from positive to negative when the rainfall

Earth Surf. Dynam. Discuss., https://doi.org/10.5194/esurf-2018-15
Manuscript under review for journal Earth Surf. Dynam.
Discussion started: 28 February 2018

duration is about 6000s.

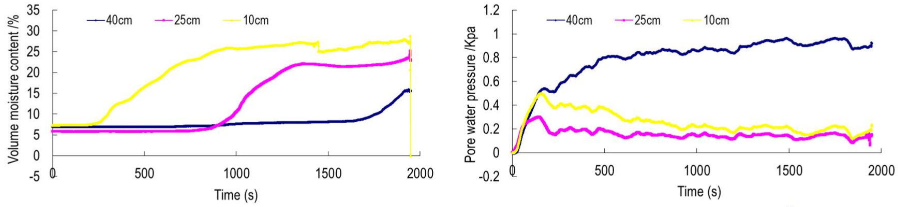

Fig. 3 Volume moisture content and pore water pressure when initial dry density of 1.54g/cm^3

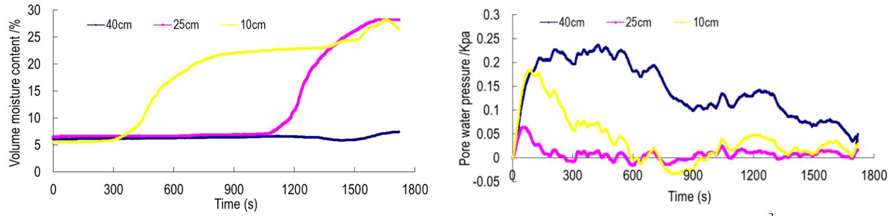

Fig. 4 Volume moisture content and pore water pressure when initial dry density of 1.63g/cm^3

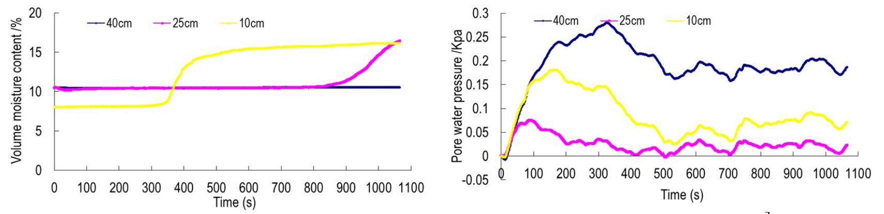

Fig. 5 Volume moisture content and pore water pressure when initial dry density of 1.72g/cm^3

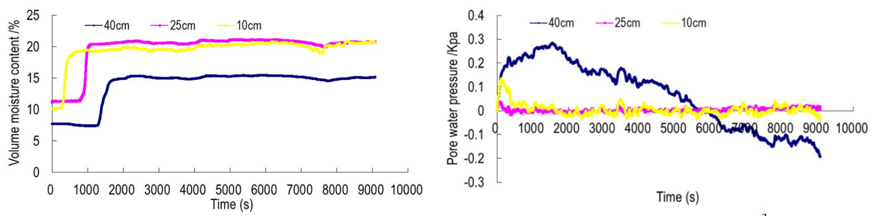

Fig. 6 Volume moisture content and pore water pressure when initial dry density of 1.81g/cm^3

3.2 Macro and micro property of gravel soil

When the initial dry density of gravel soil is 1.54~1.72g/cm^3, the landslide can be triggered by rainfall; however, the initiating processes of landslides have their similarity and difference. The similarity is that at the beginning of rainfall, the shallow soil is compacted due to the seepage force of rainfall (Fig. 7 (a)). In addition, surface runoff cannot be observed during the rainfall duration, while the muddy water can be generated and overflow the slope foot (Fig. 7 (b)). This phenomenon indicates that all the rainfall can seep into the internal soil; the fine particles (mainly clay and silt) along the seepage paths start to migrate and are attributed to the formation of the subsurface flow inside the slope. This migration process results in the variation and redistribution of the soil micro-structure (Chen et al., 2004; Zhuang et al., 2015). The difference of initiating process is that the time and pattern. For example, when the initial dry density is 1.54~1.63g/cm^3, the initiating time of landslide is 30~40 minutes. The steps of landslide initiation are as follows: first, the soil of the superficial layer slowly slides in the shape of soil flow (Fig.8 (a)); second, a small-scale slip occurs (Fig.8 (b)); third, the large-scale slide of soil is motivated (Fig.8 (c)). When the initial dry density is 1.72g/cm^3, the initiating time of landslide is 18 minutes. Before landslide initiation, firstly, the shear opening occurs accompanied by the cracks developing in the slope foot (Fig. 9 (a)); secondly, some cracks develop inside the top of the slope (Fig. 9 (b)); finally, landslide initiates

Earth Surf. Dynam. Discuss., https://doi.org/10.5194/esurf-2018-15
Manuscript under review for journal Earth Surf. Dynam.
Discussion started: 28 February 2018

Earth Surface Dynamics
Discussions
Open Access

accompanied by the instantaneous expansion of cracks (Fig. 9 (c)), which takes 5s. This initiation process implies that when the fine particles migrate, the particles in the framework start to move in translation and rotation under the action of gravity, and fill the interval space and block the downstream channels of the seepage path. All the above process can lead to the decrease of the void ratio and the increase of the pore water pressure, and result in the formation of sliding fracture surface (Gao et al., 2011). When the initial dry density is 1.81g/cm^3, the slope keeps stable and landslide cannot be triggered by the rainfall even though the fine particles disappear, and the coarse particles are exposed at the slope surface.

(a) (b)

Fig.7 Similarity of process of landslide initiation

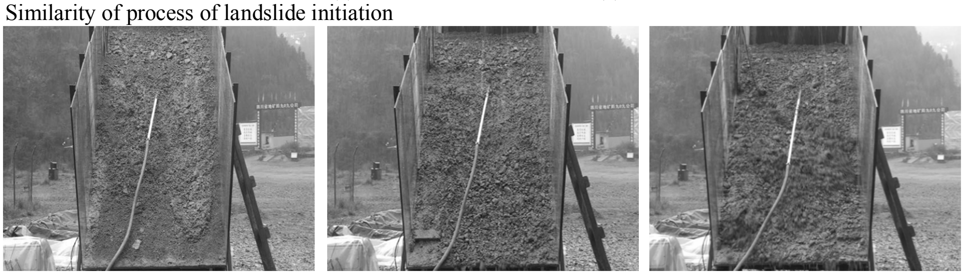

(a) (b) (c)

Fig. 8 Process of landslide initiation (initial dry density of 1.54~1.63g/cm^3)

(a) (b) (c)

Fig. 9 Process of landslide initiation (initial dry density of 1.72g/cm^3)

As shown in Tab.2, when the initial dry density is 1.54~1.72g/cm^3, the natural density and dry density of soil depth of 5cm~20cm (line 1#, 2# and 3#) are larger than those before the test, and the void ratio is smaller than it before the test. Among these three lines, the rate of change of natural density and dry density in line 1# is the highest. When the initial dry density is 1.63cm^3, the dry density of soil depth of 40cm (line 3#) is smaller than it before the test, and the void ratio is larger than it before the test. When the initial dry density is 1.81g/cm^3, the natural density and dry density increase after the test.

Tab 2. Density and void ratio of gravel soil with initial dry density 1.54~1.81g/cm^3

Number	Initial dry density (g/cm^3)	Line number	h (cm)	Natural density of soil close to failure ρ (g/cm^3)	Mass moisture content ω (%)	Dry density of soil close to failure ρ_d (g/cm^3)	Void ratio close to failure $e=G_s/\rho_d$-1	$\sigma_z=\gamma h$ (Kpa)	$\sigma_x=\sigma_y=K_a\gamma h$ (Kpa)	$p'=(\sigma_x+\sigma_y+\sigma_z)/3$ (Kpa)
1	1.54	3#	5	2.08±0.05	9.35±0.85	1.90±0.04	0.39±0.03	1.04	0.59	0.74
		3#	28	1.93±0.03	8.61±1.16	1.77±0.02	0.49±0.02	5.39	3.07	3.84
		2#	33	2.07±0.05	9.15±0.15	1.89±0.04	0.40±0.03	6.82	3.88	4.86
		1#	21	2.10±0.05	9.63±1.01	1.91±0.05	0.39±0.04	4.40	2.51	3.14
2	1.63	3#	5	2.19±0.01	13.36±0.09	1.98±0.01	0.34±0.01	0.44	0.25	0.31
		3#	40	1.67±0.03	6.15±0.17	1.58±0.02	0.68±0.02	6.68	3.80	4.76
		2#	20	2.09±0.04	10.18±0.21	1.90±0.04	0.39±0.03	4.19	2.38	2.99
		1#	13	2.23±0.04	10.84±0.83	2.01±0.02	0.32±0.02	2.90	1.65	2.07
3	1.72	3#	10	2.22±0.02	8.45±0.72	2.05±0.02	0.30±0.01	2.22	1.26	1.58
		3#	25	2.34±0.04	8.59±0.261	2.16±0.05	0.23±0.03	5.86	3.33	4.17
		1#	10	2.30±0.01	9.26±0.42	2.10±0.01	0.26±0.01	2.30	1.31	1.64
4	1.81	3#	5	2.14±0.04	9.57±0.75	1.95±0.04	0.36±0.03	1.28	0.73	0.91
		3#	10	2.26±0.01	8.16±0.39	2.09±0.02	0.27±0.01	2.26	1.28	1.61

As shown on the section 2.2.1, P_5 of soil before the test is 55.32%; therefore, the coarse particles and the fine particles interact with each other to form the soil structure, which influence the changes of the dry density (Guo 1998) and landslide or debris flow characteristics (Li et al., 2014). In order to find out the reasons for the variation of dry density and void ratio, P_5, $P_{0.075}$ and P_2 of line 1# and 3# before and after tests are compared. As shown in Tab.3, in the condition of the same initial dry density, when the initial dry density is 1.54g/cm^3 and 1.63g/cm^3, the loss of $P_{0.075}$ is the largest in the shallow layer of the slope top, followed by the loss of $P_{0.075}$ in the slope foot. It is indicated that in the early period of rainfall, at the slope top, the fine particles of the shallow soil mainly migrate along the direction of gravity; when the interflow forms, the fine particles begin to move to the slope foot. This process results in the porosity at the migration position increases, while the porosity of the position which is filled by fine particles decreases (Wang et al., 2010). It is also regarded as the seepage-compacting effect (Jiang et al., 2013). As a result, the shallow soil on the slope top is looser than the shallow soil on the slope foot. The loss of $P_{0.075}$ at the slope top decreases significantly with depth. Especially, it is about -1.26% at the depth of 40cm. It is indicated that the depth of rainfall infiltration is about 40 cm. When the range of the initial dry density are 1.72g/cm^3~1.81g/cm^3, with the increase of depth, the variation of $P_{0.075}$ at the slope top changes from negative to positive. This trend indicates that the fine particles migrate and deposit at the depth of 5~25cm wherein the depth is 10~25cm, 5~10cm for the initial dry density of 1.72g/cm^3 and 1.81g/cm^3.

Tab 3. Variation of coarse and fine particles contents

Number	Initial dry density (g/cm^3)	Line number	h (cm)	P_5	ΔP_5	$P_{0.075}$	$\Delta P_{0.075}$	P_2	ΔP_2
1	1.54	3#	5	61.00%	10.25%	0.66%	-76.24%	30.69%	-0.16%
		3#	28	55.91%	1.05%	2.01%	-27.90%	34.36%	11.76%
		1#	21	58.98%	6.60%	0.77%	-72.36%	31.07%	1.05%
2	1.63	3#	5	58.69%	6.09%	0.91%	-67.23%	31.40%	2.15%
		3#	40	57.98%	4.80%	2.75%	-1.26%	31.69%	3.07%
		1#	13	67.66%	22.30%	1.26%	-54.81%	26.23%	-14.68%
3	1.72	3#	5	55.98%	1.18%	1.03%	-62.98%	32.70%	6.38%
		3#	10	54.01%	2.37%	1.78%	-36.14%	33.94%	10.40%
		3#	25	55.32%	0%	3.17%	13.85%	34.05%	10.75%

		1#	10	56.15%	1.5%	1.42%	-49.09%	33.67%	9.53%
4	1.81	3#	5	52.50%	-5.11%	2.06%	-25.83%	35.49%	15.45%
		3#	10	52.55%	-5.01%	2.86%	2.68%	33.91%	10.30%

Note: the positive value of the change represents an increase while the negative value represents a decrease.

On the slope top, the trend of P_5 (the depth of 5cm) is from positive to negative with the increasing of initial dry density, which range is from -5.11% to 10.25%. The reason is that the loss of fine particles contributes to the relatively increase of the coarse particles' content. The overall trend of $P_{0.075}$ at the slope top and slope foot both decreases, which range is from 25.83% to 76.24% and from 49.09% to 72.36% respectively. The relationship between the loss of $P_{0.075}$ ($\Delta P_{0.075}$, which is negative) at the slope top and slope foot and initial dry density ρ_d is shown in Fig. 10. The regression equation is as follows: $\Delta P_{0.075}$=1.2632ρ_d - 2.6464, $\Delta P_{0.075}$=1.709ρ_d - 3.4391, and R^2 is 0.8827, 0.8199 respectively. It is indicating that $\Delta P_{0.075}$ has the significant correlation with ρ_d; specially, the greater initial dry density, the smaller loss of $P_{0.075}$. When ρ_d is 1.53g/cm^3, P_2 decreases and the amount of change is -0.16%, while ρ_d is 1.63~1.81g/cm^3, P_2 increases with the range of 2.15%~15.45%. The reason for the loss of $P_{0.075}$ and P_2 is that the fine particles, including silt and clay, are continuously motivated to move by the subsurface flow. The reason for the increase of P_2 might be that during the rainfall, the large gravels keep rolling off, so that the content of particles larger than 2 mm decreases, so that the content of particles smaller than 2 mm relatively increases.

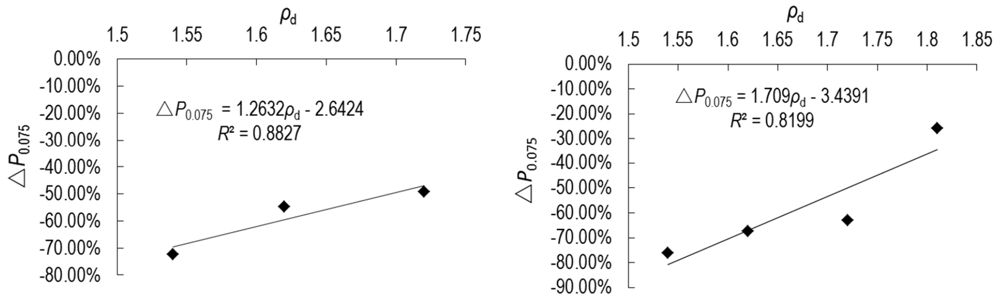

(a) Slope foot (b) Slope top

Fig. 10 Relationship between $\Delta P_{0.075}$ and ρ_d

3.3 Critical state of gravel soil

(1) Definition of critical state and calculation of porosity ratio

Casagrande et al pointed out under the condition of continuous shear load, the constant state of the deviation stress and the void ratio are the critical state (Casagrande A 1936; Roscoe et al., 1963; Schofield and Wroth 1968). For the consolidation drainage test, under a certain confining pressure, as the axial strain ε_a increases, the principal stress q and the volume strain ε_v tends to a stable value, at this time the soil is in a critical state characterized by the plastic flow (Liu et al., 2011). According to the results of triaxial shear tests, when the axial strain reaches 16%, the deviation stress is stable, and the absolute value of the increment of volume change to the current volume change is less than 0.01; the soil enters the critical state (Liu et al., 2012). A certain relationship between the void ratio and the volumetric strain exists in sand and gravel soil, so that the current porosity ratio e is calculated by formula (2) (Xu et al., 2009), wherein e_0 is the initial void ratio.

$$e = (1 + e_0)\exp(-\varepsilon_v) - 1 \tag{2}$$

(2) The critical line in the e_c- p' plane

Tab. 4 shows the critical void ratio e_c, q and p' under two initial dry densities. As shown in Table 4, the same critical void ratio will be reached approximately for the gravel soil with initial dry density of 1.94g/cm^3 and 2.00g/cm^3. This result is consistent with existing study (Gabet and Mudd 2006; Iverson et al., 2000), which can indicate that gravel soil

Earth Surf. Dynam. Discuss., https://doi.org/10.5194/esurf-2018-15
Manuscript under review for journal Earth Surf. Dynam.
Discussion started: 28 February 2018

also has the similar principle that the soil with the same grade will shear to reach the same critical void ratio.

Tab 4. Critical void ratio e_c of gravel soils

σ_3(Kpa)	Initial dry density (g/cm^3)	e_c	q (Kpa)	p' (Kpa)
50	1.94	0.32	93.41	95.98
	2.00	0.34	69.50	84.65
100	1.94	0.30	227.43	213.80
	2.00	0.30	159.14	178.13
150	1.94	0.27	324.79	312.39
	2.00	0.29	181.12	239.86

The fitting curve of e_c and lnp' is shown in Fig. 11 (a). The correlation coefficient is 0.8566, which indicates a statistically significant relationship between e_c and p'. According to the normalized residual probability, P-value of 0.964 is greater than the selected significance level (P=0.05), which indicates that the residuals follow a normal distribution. Therefore, the mathematical expression of e_c-lnp' of gravel soil in the critical state is as follows:

$$e_c = 0.5241 - 0.04304 \ln p' \tag{3}$$

(3) The critical line in the q- p' plane

The fitting curve of q and the p' is shown in Fig. 11 (b). The correlation coefficient is 0.9465, which indicates a statistically significant relationship between q and p'. The mathematical expression of q- p' is as follows:

$$q = 0.6641(p')^{1.063} \tag{4}$$

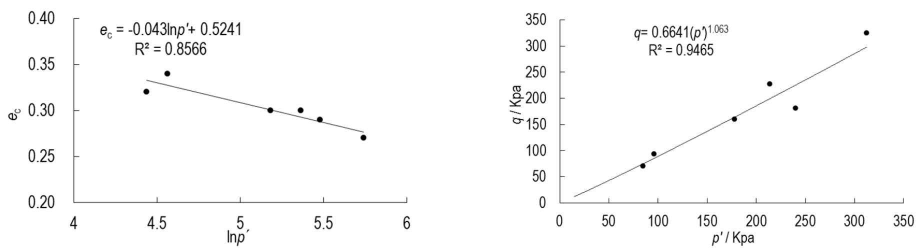

(a) e_c-lnp' (b) q-p'

Fig. 11 Critical sate line of gravel soil

4 Discussion

The relative position of the state parameter (e, p') at the critical state line is shown in Fig.12. As shown in Fig.12, when the initial dry density is 1.54g/cm^3~1.63g/cm^3, the shallow soil at the slope top, the soil inside the middle of the slope and at the slope foot dilates, while the soil with the depth 28cm and 40cm at the slope top contracts. When the initial dry density is 1.72g/cm^3~1.81g/cm^3, the soil on the slope top and slope foot both dilate. When the initial dry density is 1.81g/cm^3, the landslide cannot be triggered by the rainfall. The reasons might be that the soil is in the dense state; therefore, the permeability capacity of the soil is low and the infiltration depth is restricted; the loss of the pore water pressure due to soil dilation is difficult to recover timely, which can result in the discontinuity of the shear deformation. The results show that there are two types of dilation and contraction in the mechanical state of gravel soil when the landslide initiates; specially, dilation is the primary type.

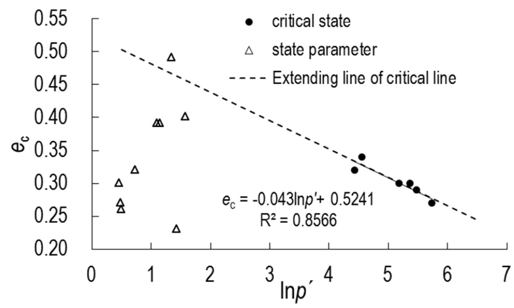

Fig.12 Mechanical property of gravel soil

During the initiating process of landslide, the gravel soil slope changes from the unsaturated state to the saturated state. Due to the increase of pore water pressure, the soil of potential sliding surface falls into the shear failure under the drainage condition; however, the shear strain is small. When the soil is damaged by shear shrinkage, the porosity decreases after the soil is destroyed; the excess pore water pressure cannot be quickly dissipated in a short period of time, which causes the pore water pressure of the soil near the damage position to increase, and contributes to the decrease of the mean effective stress. The whole process of landslide initiation exhibits a sudden characteristic.

When the soil is destroyed by shear dilation, rainfall infiltration leads to the increase of pore water pressure in the soil near the potential slip surface; a small part of soil at the slope foot begins to slip, which causes the sliding force increase; subsequently, the effective stress decreases and the shear deformation occurs. At this moment, the pore water pressure decreases; the loss of shear strength due to strain softening is restored, and the deformation of soil is stopped. If there is the sufficient infiltration of rainfall, the pore water pressure can be recovered, and the soil deformation can continue. When the soil is in a dense state (relative density D_r > 2/3), if the infiltration rate is less than the rainfall intensity, it is difficult for the soil to reach the critical state due to short-term rainfall; at this moment, the slope still keeps stable. The macroscopic phenomenon of the soil deformation is a kind of local deformation and destruction, such as circumferential cracks, partial collapse or uplift. If the infiltration rate is larger than the rainfall intensity, although the rainfall infiltration is enough to break the mechanical balance of slope, its process still needs a relatively long period of time, so the macroscopic deformation soil appears as a gradual deformation and damage, such as the multiple slides and landslide. When the soil is in a medium dense state ($1/3<D_r\leq 2/3$), the loss of the pore water pressure due to dilation will be recovered because of the rapid infiltration of rainfall, the shear deformation of soil will continue. The macroscopic phenomenon of soil deformation will appear as a kind of sudden failure (Dai et al., 2000).

5 Conclusion

(1) The timing and patterns of landslide initiations were closely related to their initial dry densities, and initiation processes were accompanied by a variation of dry density and void ratio. The overall trend is that the dry density at the depth of 5cm~20cm increases, and the void ratio decreases. The change rate at the slope foot is the largest. When the initial dry density is 1.63g/cm^3, the dry density (the depth of 40cm on the slope top) decreases, and its porosity increases.

(2) Fine particle migration in soil and coarse-fine particle content rearrangement contributed to the internal micro structure reorganization, which was supposed to be the main reason for variation of dry density and void ratio. When the initial dry density is 1.54g/cm^3 and 1.63g/cm^3, the variation of $P_{0.075}$ (the depth of 5cm at the top of the slope) is the largest, followed by the variation of $P_{0.075}$ at the slope foot. The variation trend of P_5 changes from increasing to decreasing. The loss of $P_{0.075}$ at the top of the slope decreased significantly with depth; in addition, the loss of $P_{0.075}$ at the slope top the and at the slope foot both have the positive correlation with the initial dry density. P_2 has the increase trend for the initial dry densities of 1.63~1.81g/cm^3 except 1.54g/cm^3.

(3) The same critical porosity ratio will be reached approximately for the gravel soil with initial dry density of 1.94g/cm^3 and 2.00g/cm^3.

Earth Surf. Dynam. Discuss., https://doi.org/10.5194/esurf-2018-15
Manuscript under review for journal Earth Surf. Dynam.
Discussion started: 28 February 2018

(4) The mathematical expression of e_c-lnp', q-p' of gravel soil in the critical state is as follows: $e_c=0.5241-0.04304\ln p'$, $q=0.6641(p')^{1.063}$.

(5) The relative position of the state parameter (e, p') at the critical *state* line is applied to estimate the mechanical state of gravel soil.

(6) There are two types of dilation and contraction in the mechanical properties of gravel soil when landslide initiates. In addition, dilation is the primary type.

Acknowledgements

This study was funded by the National Natural Science Foundation of China (No 41071058, 41402272, 51609041); Disaster Prevention and Mitigation and Engineering Safety Key Laboratory Project of Guangxi Province (No 2016ZDX09).

References

Been, K.and Jefferies, M.: A state parameter for sands. Geotechnique, 35, 99-112, 1985.

Casagrande A: Characteristics of cohesionless soils affecting the stability of slopes and earth fills. Journal of the Boston Society of Civil Engineers, 23, 13-32, 1936.

Chen, H. X., Zhang, L. M., Chang, D. S.and Zhang, S.: Mechanisms and runout characteristics of the rainfall-triggered debris flow in Xiaojiagou in Sichuan Province, China. Natural Hazards, 62, 1037-1057, doi: 10.1007/s11069-012-0133-5, 2012a.

Chen, N. S., Cui, P., Wang, X. Y.and Di, B. F.: Testing study on strength reduction of gravelly soil in triggering area of debris flow under earthquake. Chinese Journal of Rock Mechanics and Engineering, 23, 2743-2747, 2004 (in Chinese).

Chen, N. S., Zhou, W., Yang, C. L., Hu, G. S., Gao, Y. C.and Han, D.: The processes and mechanism of failure and debris flow initiation for gravel soil with different clay content. Geomorphology, 121, 222-230, doi: 10.1016/j.geomorph.2010.04.017, 2010.

Chen, N. S., Zhu, Y. H., Huang, Q., Lqbal, J., Deng, M. F.and He, N.: Mechanisms involved in triggering debris flows within a cohesive gravel soil mass on a slope: a case in SW China. Journal of Mountain Science, 14, 611-620, doi: 10.1007/s11629-016-3882-x, 2017.

Chen, Z. Y., Zhou, J. X.and Wang, H. J. Soil Mechanics. 19th edn. Tsinghua University Press, Beijing, 2012b.

Cui, P., Xiang, L. Z.and Zou, Q.: Risk assessment of highways affected by debris flows in Wenchuan earthquake area. Journal of Mountain Science, 10, 173-189, doi: 10.1007/s11629-013-2575-y, 2013.

Cui, P., Zhuang, J., Qi, , Chen, X. C., Zhang, J., Qiang,and Zhou, X. J.: Characteristics and countermeasures of debris flow in Wenchuan area after the earthquake. Journal of Sichuan University (Engineering Science Edition), 42, 10-19, 2010 (in Chinese).

Dai, F. C., Chen, S. Y.and Li, Z. F.: Analysis of landslide initiative mechanism based on stress-strain behavior of soil. Chinese Journal Of Geotechnical Engineering, 22, 127-130, 2000 (in Chinese).

Dai, F. C., Lee, C. F.and Wang, S. J.: Analysis of rainstorm-induced slide-debris flows on natural terrain of Lantau Island, Hong Kong. Engineering Geology, 51, 279-290, doi: S0013-7952(98)00047-7, 1999a.

Dai, F. C., Lee, C. F.and Wang, S. J.: Stress-strain behaviour of a loosely compacted voleanic-derived soil and its significance to rainfall-induced fill slope failures. Engineering Geology, 53, 359-370, doi: S0013-7952(99)00016-2, 1999b.

Fang, H., Cui, P., Pei, L. Z.and Zhou, X. J.: Model testing on rainfall-induced landslide of loose soil in Wenchuan earthquake region. Natural Hazards and Earth System Science, 12, 527-533, doi: 10.5194/nhess-12-527-2012, 2012.

Fleming, R. W., Ellen, S. D.and Algus, M. A.: Transformation of dilative and contractive landslide debris into debris flows-An example from marin County, California. Engineering Geology, 27, 201-223, 1989.

Gabet, E. J.and Mudd, S. M.: The mobilization of debris flows from shallow landslides. Geomorphology, 74, 207-218, 2006.

Gao, B., Zhou, J.and Zhang, J.: Macro-meso analysis of water-soil interaction mechanism of debris flow starting process. Chinese Journal of Rock Mechanics and Engineering, 30, 2567-2573, 2011 (in Chinese).

Guo, Q. Q: Engineering features and utilization of coarse-grained soil. 1st edn. The Yellow River Water Conservancy Press, Zhengzhou, 1998.

Hu, W., Dong, X. J., Xu, Q., Wang, G. H., Asch, T. W. J. V.and Hicher, P. Y.: Initiation processes for run-off generated debris flows in the Wenchuan earthquake area of China. Geomorphology, 253, 468-477, doi: 10.1016/j.geomorph.2015.10.024, 2016.

Hu, W., Xu, Q., Asch, T. W. J. V., Zhu, X.and Xu, Q. Q.: Flume tests to study the initiation of huge debris flows after the Wenchuan earthquake in S-W China. Engineering Geology, 182, 121-129, doi: 10.1016/j.enggeo.2014.04.006, 2014.

Huang, R. Q., Huang, J., Ju, N. P., He, C. Y.and Li, W., Le,: WebGIS-based information management system for landslides triggered by Wenchuan earthquake. Natural Hazards, 65, 1507-1517, doi: 10.1007/s11069-012-0424-x, 2012.

Huang, X.and Tang, C.: Formation and activation of catastrophic debris flows in Baishui River basin, Sichuan Province, China. Landslides, 11, 955-967, doi: 10.1007/s10346-014-0465-1, 2014.

Iverson, N. R., Mann, J. E.and Iverson, R. M.: Effects of soil aggregates on debris-flow mobilization: Results from ring-shear experiments. Engineering Geology, 114, 84-92, doi: 10.1016/j.enggeo.2010.04.006, 2010.

Iverson, R. M.: Landslide triggering by rain infiltration. Water Resources Research, 36, 1897-1910, 2000.

Iverson, R. M.: Regulation of landslide motion by dilatancy and pore pressure feedback. Journal of Geophysical Research: Earth Surface, 110, 1-16, doi: 10.1029/2004JF000268, 2005.

Iverson, R. M., Reid, M. E., Iverson, N. R., LaHusen, R. G.and Logan, M.: Acute sensitivity of landslide rates to initial soil porosity. Science, 290, 513-516, doi: 10.1126/science.290.5491.513, 2000.

Iverson, R. M., Reid, M. E.and Lahusen, R. G.: Debris-flow mobilization from landslides. Annual Review of Earth & Planetary Sciences, 25, 85-138, 1997.

Jiang, Z. M., Wang, W., Feng, S. R.and Zhong, H. Y.: Experimental of study on the relevance between stress state and seepage failure of sandy-gravel soil. Shuili Xuebao, 44, 1498-1505, 2013 (in Chinese).

Li, Y., Liu, J. J., Su, F. H., Xie, J.and Wang, B. L.: Relationship between grain composition and debris flow characteristics: a case study of the Jiangjia Gully in China. Landslides, 12, 19-28, doi: 10.1007/s10346-014-0475-z, 2014.

Li, Y. F., Wang, Z. Y., Shi, W. J.and Wang, X. Z.: Slope debris flows in the Wenchuan Earthquake area. Journal of Mountain Science, 7, 226-233, doi: 10.1007/s11629-010-2014-2, 2010.

Liu, D. L., Zhang, S. J., Yang, H. J., Zhao, L. Q., Jiang, Y. H., Tang, D.and Leng, X. P.: Application and analysis of debris-flow early warning system in Wenchuan earthquake-affected area. Natural Hazards and Earth System Sciences, 16, 483-496, doi: 10.5194/nhess-16-483-2016, 2016.

Liu, E. L., Chen, S. S.and Li, G. Y.: Critical state of rockfill materials and a constitutive model considering grain crushing. Rock and Soil Mechanics, 32, 148-154, 2011 (in Chinese).

Liu, E. L., Qin, Y. L., Chen, S. S.and Li, G. Y.: Investigation on critical state of rockfill materials. Shuili Xuebao, 43, 505-511, 519, 2012 (in Chinese).

Ma, C., Hu, K. H., Zou, Q.and Tian, M.: Characteristics of clustering debris flows in Wenchuan earthquake zone. Journal of Mountain Science, 10, 953-961, doi: 10.1007/s11629-013-2410-5, 2013.

McKenna, J. P., Santi, P. M., Amblard, X.and Negri, J.: Effects of soil-engineering properties on the failure mode of shallow landslides. Landslides, 9, 215-228, doi: 10.1007/s10346-011-0295-3, 2011.

Ni, H. Y., Tang, C., Zheng, W. M., Xu, R. G., Tian, K.and Xu, W.: An Overview of Formation Mechanism and Disaster Characteristics of Post-seismic Debris Flows Triggered by Subsequent Rainstorms in Wenchuan Earthquake Extremely Stricken Areas. Acta Geologica Sinica-English Edition, 88, 1310-1328, doi: 10.1111/1755-6724.12290, 2014.

Qu, Y. P., Tang, C., Wang, J. L., Tang, H. X., Liu, Y., Chen, H. L.and Huang, W.: Debris flow initiation mechanisms in strong earthquake area. Mountain Research, 30, 336-341, doi: 10.16089/j.cnki.1008-2786.2012.03.013, 2012 (in Chinese).

Roscoe, K. H., Schofield, A. N.and Thuraijajah, A.: Yielding of clays in states wetter than critical. Geotechnique, 13, 211-240, 1963.

Sassa, K.: The mechanism to initiate debris flows as undrained shear of loose sediments. Internationales Symposium Interpraevent, 73-87, 1984.

Schofield, A. N.and Wroth, C. P: Critical state soil mechanics. University of Cambridge, 1968.

Schulz, W. H., McKenna, J. P., Kibler, J. D.and Biavati, G.: Relations between hydrology and velocity of a continuously moving landslide - evidence of pore-pressure feedback regulating landslide motion? Landslides, 6, 181-190, doi: 10.1007/s10346-009-0157-4, 2009.

Sun, P., Zhang, Y. S., Shi, J. S.and Chen, L. W.: Analysis on the dynamical process of Donghekou rockslide-debris flow triggered by 5.12 Wenchuan earthquake. Journal of Mountain Science, 8, 140-148, doi: 10.1007/s11629-011-2112-9, 2011.

Tang, C., Li, W. L., Ding, J.and Huang, X. C.: Field Investigation and Research on Giant Debris Flow on August 14, 2010 in Yingxiu Town, Epicenter of Wenchuan Earthquake. Earthscience- Journal of China University of Geosciences, 36, 172-180, 2011a, (in Chinese).

Tang, C.and Liang, J. T.: Characteristics of debris flows in Beichuan epicenter of the Wenchuan earthquake triggered by rainstorm on september 24, 2008. Journal of Engineering Geology, 16, 751-758, doi: 10.1016/j.geomorph.2005.08.013, 2008 (in Chinese).

Tang, C., Zhu, J., Chang, M., Ding, J.and Qi, X.: An empirical-statistical model for predicting debris-flow runout zones in the Wenchuan earthquake area. Quaternary International, 250, 63-73, doi: 10.1016/j.quaint.2010.11.020, 2012.

Tang, C., Zhu, J., Ding, J., Cui, X. F., Chen, L.and Zhang, J. S.: Catastrophic debris flows triggered by a 14 August 2010 rainfall at the epicenter of the Wenchuan earthquake. Landslides, 8, 485-497, doi: 10.1007/s10346-011-0269-5, 2011b.

Tang, C., Zhu, J., Li, W. L.and Liang, J. T.: Rainfall-triggered debris flows following the Wenchuan earthquake. Bulletin of Engineering Geology and the Environment, 68, 187-194, doi: 10.1007/s10064-009-0201-6, 2009.

Verdugo, R.and Ishihara, K.: The steady state of sandy soils. Soil and Foundation, 36 81-91, doi: 1996.

Wang, G. H.and Sassa, K.: Pore-pressure generation and movement of rainfall-induced landslides:effects of grainsize and fine-particle content. Engineering Geology, 69, 109-125, doi: 10.1016/S0013-7952(02)00268-5, 2003.

Wang, J., Yu, Y., Pan, H. L., Qiao, C.and Ou, G. Q.: Debris flow formation process and critical hydrodynamic conditions in the meizoseismal area of the Wenchuan earthquake. Journal of Mountain Science, 12, 699-710, doi: 10.1007/s11629-014-3370-0, 2015.

Wang, Z. B., Wang, N., Hu, M. J.and Chen, Z. X.: Characteristics of gravelly soil and their implications for slope instability in Jiangjiagou ravine. Rock and Soil Mechanics, 31, 206-211, 2010 (in Chinese).

Xie, H., Zhong, D. L., Jiao, Z.and Zhang, J. S.: Debris flow in Wenchuan quake-hit area in 2008. Mountain Research, 27, 501-509, 2009 (in Chinese).

Xu, Q., Zhang, S., Li, W. L.and Asch , T. W. J. V.: The 13 August 2010 catastrophic debris flows after the 2008

Earth Surf. Dynam. Discuss., https://doi.org/10.5194/esurf-2018-15
Manuscript under review for journal Earth Surf. Dynam.
Discussion started: 28 February 2018

Wenchuan earthquake, China. Natural Hazards and Earth System Sciences, 12, 201-216, doi: 10.5194/nhess-12-201-2012, 2012.

Xu, S. H., Zheng, G.and Xu, G. L.: Critical state constitutive model of sand with shear hardening. Chinese Journal of Geotechnical Engineering, 31, 953-958, 2009 (in Chinese).

Yin, Y. P., Cheng, Y. L., Liang, J. T.and Wang, W. P.: Heavy-rainfall-induced catastrophic rockslide-debris flow at Sanxicun, Dujiangyan, after the Wenchuan Ms 8.0 earthquake. Landslides, 13, 9-23, doi: 10.1007/s10346-015-0554-9, 2016.

You, Y., Liu, J. F., Chen, X. Z.and Pan, H. L.: Debris flow formation conditions and optimal characteristics of drainage canal following Wenchuan earthquake. Environmental Earth Sciences, 65, 1005-1012, doi: 10.1007/s12665-011-1024-x, 2012.

YU, B., Ma, Y.and Wu, Y. F.: Investigation of serve debris flow hazards in Wenjia gully of Sichuan province after the Wenchuan earthquake. Jouranl of Enigeering Geology, 18, 827-836, 2010 (in Chinese).

Zhang, M., Hu, R. L.and Yin, Y. P.: Study of transform mechanism of landslide-debris flow with ring shear test. Chinese Journal of Rock Mechanics and Engineering, 29, 822-832, 2010 (in Chinese).

Zhang, S.and Zhang, L. M.: Impact of the 2008 Wenchuan earthquake in China on subsequent long-term debris flow activities in the epicentral area. Geomorphology, 276, 86-103, doi: 10.1016/j.geomorph.2016.10.009, 2017.

Zhang, S., Zhang, L. M., Chen, H. X., Yuan, Q.and Pan, H.: Changes in runout distances of debris flows over time in the Wenchuan earthquake zone. Journal of Mountain Science, 10, 281-292, doi: 10.1007/s11629-012-2506-y, 2013.

Zhang, Y. S., Cheng, Y. L., Yin, Y. P., Lan, H. X., Wang, J.and Fu, X. X.: High-position debris flow: A long-term active geohazard after the Wenchuan earthquake. Engineering Geology, 180, 45-54, doi: 10.1016/j.enggeo.2014.05.014, 2014.

Zhou, G. G. D., Cui, P., Tang, J. B., Chen, H. Y., Zou, Q.and Sun, Q. C.: Experimental study on the triggering mechanisms and kinematic properties of large debris flows in Wenjia Gully. Engineering Geology, 194, 52-61, doi: 10.1016/j.enggeo.2014.10.021, 2015.

Zhou, W.and Tang, C.: Rainfall thresholds for debris flow initiation in the Wenchuan earthquake-stricken area, southwestern China. Landslides, 11, 877-887, doi: 10.1007/s10346-013-0421-5, 2013.

Zhou, W., Tang, C., Asch, T. W. J. V.and Zhou, C. H.: Rainfall-triggering response patterns of post-seismic debris flows in the Wenchuan earthquake area. Natural Hazards, 70, 1417-1435, doi: 10.1007/s11069-013-0883-8, 2014.

Zhu, J., Ding, J.and Liang, J. T.: Influences of the Wenchuan Earthquake on sediment supply of debris flows. Journal of Mountain Science, 8, 270-277, doi: 10.1007/s11629-011-2114-7, 2011.

Zhu, Y. Y., Cui, P.and Chen, X. Q.: Experiment on mechanism of slope failure of debris flow fan and stability analysis. Chinese Journal of Rock Mechanics and Engineering, 24, 3927-3934,: 2005 (in Chinese).

Zhuang, J. Q., Cui, P., Hu, K. H.and Chen, X. Q.: Fine particle size moving and its effective on debris flow initiation. Mountain Research, 33, 713-720, 2015 (in Chinese).

Zhuang, J. Q., Cui, P., Peng, J. B., Hu, K. H.and Lqbal, J.: Initiation process of debris flows on different slopes due to surface flow and trigger-specific strategies for mitigating post-earthquake in old Beichuan County, China. Environmental Earth Sciences, 68, 1391-1403, doi: 10.1007/s12665-012-1837-2, 2012.